



ELSEVIER

Available online at www.sciencedirect.com

SCIENCE @ DIRECT®

Journal of Computational Physics 207 (2005) 769–787

JOURNAL OF
COMPUTATIONAL
PHYSICS

www.elsevier.com/locate/jcp

Algorithm refinement for stochastic partial differential equations: II. Correlated systems

Francis J. Alexander ^{a,*}, Alejandro L. Garcia ^b, Daniel M. Tartakovsky ^c

^a *CCS-3, Los Alamos National Laboratory, MS-B256, Los Alamos, NM 87545, USA*

^b *Department of Physics, San Jose State University, San Jose, CA 95192-0106, USA*

^c *Theoretical Division, Los Alamos National Laboratory, Los Alamos, NM 87545, USA*

Received 9 June 2004; received in revised form 28 January 2005; accepted 2 February 2005

Available online 14 April 2005

Abstract

We analyze a hybrid particle/continuum algorithm for a hydrodynamic system with long ranged correlations. Specifically, we consider the so-called train model for viscous transport in gases, which is based on a generalization of the random walk process for the diffusion of momentum. This discrete model is coupled with its continuous counterpart, given by a pair of stochastic partial differential equations. At the interface between the particle and continuum computations the coupling is by flux matching, giving exact mass and momentum conservation. This methodology is an extension of our stochastic Algorithm Refinement (AR) hybrid for simple diffusion [F. Alexander, A. Garcia, D. Tartakovsky, Algorithm refinement for stochastic partial differential equations: I. Linear diffusion, *J. Comput. Phys.* 182 (2002) 47–66]. Results from a variety of numerical experiments are presented for steady-state scenarios. In all cases the mean and variance of density and velocity are captured correctly by the stochastic hybrid algorithm. For a non-stochastic version (i.e., using only deterministic continuum fluxes) the long-range correlations of velocity fluctuations are qualitatively preserved but at reduced magnitude.

© 2005 Elsevier Inc. All rights reserved.

1. Introduction

Over the last decade, numerical methods that couple particle and continuum algorithms, commonly referred to as Algorithm Refinement (AR), have been developed. These hybrid schemes reduce the computational cost of simulating physical processes that span several length and time scales in gas [1–5], liquid [6–10], solid [11–14], mixed phase [15], and reactive systems [16]. AR hybrids are ideal for simulating

* Corresponding author.

E-mail address: fja@lanl.gov (F.J. Alexander).

physical systems in which some regions of space require a more detailed description of the physical phenomena than other regions. An example is a gas flow with a region of strong shock. The gas flow can be modelled accurately by the partial differential equations (PDEs) of hydrodynamics (e.g., Navier–Stokes PDE) away from the shock, but requires a kinetic level description, the Boltzmann (integro-differential) equation, in the shock region. The basic idea of the AR hybrid approach is to carry out detailed calculations using the fine-grained, typically expensive algorithm, only where absolutely required and then to couple this computation to a coarse-grained, less expensive method, which is used in the rest of the spatial domain.

As these AR hybrids gain popularity in applications, it is important to understand their strengths and weaknesses. This is especially true for stochastic, non-linear systems, such as those undergoing phase transitions, nucleation, noise driven instabilities, or chemical reactions. In these situations the non-linearities can exponentially modify the strength of the fluctuations in the regions of interest. Furthermore, the magnitude of fluctuations can have an exponential effect on the phenomenon of interest (e.g., first-passage time [17]). For accurate modelling of these problems, one must ensure that the noise is properly generated, propagated and dissipated. Particle methods and continuum methods treat noise in very different ways. In particle systems the inherent dynamics creates spontaneous fluctuations, for example the density in a region fluctuates as particles enter and leave. For continuum methods one typically has to solve a stochastic partial differential equation containing the appropriate noise terms (e.g., see [18]). The challenge is to ensure that the numerical method used to couple the particle and continuum computations does not adversely impact the underlying physics.

This is the second in a series of papers dealing with the issue of noise in hybrids. In the first paper [19], we concentrated on hybrids for linear processes, formulating a hybrid particle/continuum method for linear (Fickian) diffusion. The particles (independent random walkers) were coupled to a fluctuating diffusion equation. This equation was solved by finite difference methods with both deterministic and white-noise fluxes. At the interface between the particle and continuum regions the coupling was carried out by flux matching. This guaranteed strict mass conservation and yielded favorable numerical stability. Results from a variety of computational experiments were presented for both steady-state and time-dependent scenarios. In all cases the mean and variance of density were captured correctly by the stochastic AR hybrid. For a non-stochastic version (i.e., using only deterministic continuum fluxes) the mean density was reproduced correctly, but the variance was significantly under-estimated except in particle regions away from the interface.

While the first paper showed that particle/continuum AR hybrids could accurately model hydrodynamic fluctuations for the case of simple diffusion this only gives us confidence in the methodology for *linear systems*. While linear systems are important they do not exhibit certain phenomena, such as long range correlations in the field variables. For highly non-linear equations or for systems with more general multiplicative noises, deterministic hybrids are not guaranteed to yield mean values that are correct across the coupling interface, even in equilibrium. In these cases great care must be taken in the construction of the hybrid; renormalized noises or effective potentials (from which the PDE is derived) may prove useful.

In this second paper, we consider a system that intrinsically has long-range spatial correlations due to the non-linearity of its stochastic fluxes. Specifically, we consider the train model [20] for viscous transport in a gas. The train model is one of a general class of random walk models that exhibit these long-range correlations; other models include lattice gases [21] and the Knudsen chain [22]. Furthermore, these long-range correlations are generic to realistic hydrodynamic systems as predicted by a variety of theoretical approaches and confirmed by numerical simulations and laboratory experiments [23–25].

The train model is chosen because the particle and continuum representations can be constructed analytically and solved numerically. The challenge is to formulate an AR hybrid that couples the particle and continuum algorithms and show that it preserves the long-range correlations of velocity fluctuations found in the train model. This is shown to be possible for an AR hybrid using a stochastic PDE for the continuum

portion of the simulation. Surprisingly, even when a deterministic PDE is used the qualitative nature of the correlations is preserved, though at a reduced amplitude.

This paper is organized as follows: In Section 2, we present the kinetic theory formulation of the train model. Section 3 contains a description of the model in the continuum limit. Each of those sections also presents simple schemes for numerically simulating the particle and continuum representations of the train model. The Algorithm Refinement hybrid that couples the particle and continuum schemes is described in Section 5. That section also presents the results of our numerical investigations of this hybrid, comparing it with the continuum and particle simulations as well as with the theoretical results obtained in Section 4. We conclude in Section 6 with a recap of our results and implications for hybrids for correlated systems. Appendix A contains algebraic expressions for various cross-correlation terms. Appendix B is the errata for [19].

2. Discrete train model

Consider the following simple model, attributed to Tait [20], for viscous transport in a gas. Two railroad cars travel alongside each other on parallel tracks with initial velocities v_a and v_b . The train cars initially have N_a and N_b passengers, respectively; the passengers have mass m while the mass of the cars is negligible. Passengers jump at random between the trains at a rate $1/\tau$, where τ is the mean free time between a passenger's jumps to an adjacent train. When a passenger jumps from train a to train b, the exchange of momentum is mv_a , so that the trains' new velocities are

$$v'_a = \frac{mN_a v_a - mv_a}{m(N_a - 1)} = v_a; \quad v'_b = \frac{mN_b v_b + mv_a}{m(N_b + 1)} = \frac{N_b}{N_b + 1} v_b + \frac{1}{N_b + 1} v_a. \tag{1}$$

Similar to the Ehrenfest dog-flea model [26,27], this random process reaches a steady state in the long time limit. Specifically, symmetry and conservation considerations show that the mean number of passengers on each train car at steady state is $(N_a + N_b)/2$, and the mean velocity is $(N_a v_a + N_b v_b)/(N_a + N_b)$.

The train model is more interesting when we consider a set of cars on M parallel tracks, as shown in Fig. 1. Passengers on the trains jump left or right with equal probability, as in the unbiased random walk.

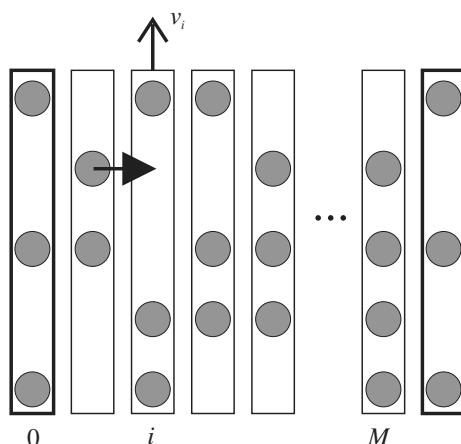


Fig. 1. Schematic illustration of the train model with M trains plus two platforms. A passenger on train $i - 1$ is shown jumping to train i , which changes velocity v_i .

Adjacent to the first and last tracks are “platforms” moving with constant numbers of passengers, N_0 and N_{M+1} , at constant velocities, v_0 and v_{M+1} ; these platforms act as reservoirs of passengers. Note that passengers on the platforms jump at half the rate of train passengers since they can only jump in one direction. At the steady state, the mean number of passengers on a train is $\langle N_i \rangle = N_0 + (N_{M+1} - N_0)i/(M + 1)$, that is, a linear profile. The mean velocity is

$$\langle v_i \rangle = \frac{\langle N_i v_i \rangle}{\langle N_i \rangle} = \frac{N_0 v_0 + (N_{M+1} v_{M+1} - N_0 v_0)i/(M + 1)}{N_0 + (N_{M+1} - N_0)i/(M + 1)}, \quad (2)$$

since the mean momentum profile is linear. Note that if the platforms have equal numbers of passengers then the velocity profile is also linear, as in Couette shear flow.

Our interest in this model lies in its fluctuations in general, and in the long-range correlations of velocity fluctuations in particular. An earlier study of this model [28] demonstrated that these correlations are long-ranged and very similar to those observed in a dilute gas under shear [24]. Specifically, when the mean density is constant (i.e., $N_0 = N_{M+1}$) this correlation is piece-wise linear

$$\langle \delta v_i \delta v_j \rangle = \frac{(v_{M+1} - v_0)^2}{N_0(M + 1)^3} \begin{cases} i(M + 1 - j) & i \leq j, \\ j(M + 1 - i) & i > j. \end{cases} \quad (3)$$

When $N_0 \neq N_{M+1}$, the correlations are also long-ranged but have a more complicated form (see Section 4). Similar long-range correlations of fluctuations are observed in a dilute gas subjected to a shear [24] as well as many other non-equilibrium systems [23].

The train model is very simple to simulate numerically, being only slightly more complicated than the basic random walk. Starting from an initial state, a random passenger is chosen to jump in a random direction. A passenger jumping onto a train changes the velocity of that train. If the passenger jumps from a platform onto a train, a new passenger is added to the system; vice versa a passenger is removed. After each jump the time is advanced by $(\tau/N_\Sigma)\mathfrak{R}_e$, where N_Σ is the total number of passengers in the system and \mathfrak{R}_e is an exponentially distributed random number. This algorithm is discussed in further detail in [28].

3. Continuum train model

The train model, as presented in the previous section, is a discrete random-walk process. As our interest is in particle/continuum hybrids, the next step is to formulate the continuum train model and a numerical scheme for solving the resulting SPDE. We start with the following general expressions for the continuum PDEs for the train model:

$$\frac{\partial \rho}{\partial t} = -\frac{\partial}{\partial x} F(\rho); \quad \frac{\partial p}{\partial t} = -\frac{\partial}{\partial x} G(\rho, v), \quad (4)$$

where $\rho(x, t)$ is the mass density, F is the mass flux, $p(x, t)$ is the momentum, G is the momentum flux, and $v = p/\rho$ is the fluid velocity. These equations arise from the continuum limit of the integral construction of flux conservation. Stepping back to this more fundamental construction, we formulate the density equation as

$$\frac{\rho_{i;n+1} - \rho_{i;n}}{\Delta t} = -\left(\frac{(F_{i;n}^{+\rightarrow} - F_{i;n}^{+\leftarrow}) - (F_{i;n}^{-\rightarrow} - F_{i;n}^{-\leftarrow})}{\Delta x} \right), \quad (5)$$

where $\rho_{i;n} = \rho(x_i, t_n)$ with $x_i = (i - \frac{1}{2})\Delta x$, $i = 1, \dots, M$, and $t_n = n\Delta t$, $n = 0, 1, \dots$. The superscript + (or -) indicates that the flux is through the side between cells i and $i + 1$ (or $i - 1$); the superscript \rightarrow (or \leftarrow) indicates

that the term is the flux contribution due to particles moving left-to-right (or right-to-left). Note that if we associate a grid point with a single discrete train then $N_i = \rho_i \Delta x / m$.

Similarly, the discretization for the momentum equation gives

$$\frac{P_{i;n+1} - P_{i;n}}{\Delta t} = - \left(\frac{(G_{i;n}^{+\rightarrow} - G_{i;n}^{+\leftarrow}) - (G_{i;n}^{-\rightarrow} - G_{i;n}^{-\leftarrow})}{\Delta x} \right). \tag{6}$$

These equations are discretized in a slightly different fashion than in [19] where we used $F_{i;n}^+ = F_{i;n}^{+\rightarrow} - F_{i;n}^{+\leftarrow}$ and $F_{i;n}^- = F_{i;n}^{-\rightarrow} - F_{i;n}^{-\leftarrow}$. The reason for introducing this more complicated construction is that the momentum fluxes cannot be specified by our previous construction. Specifically, particles crossing an interface from left-to-right carry a different momentum from those going right-to-left (i.e., mass diffusion is simpler since particles always carry the same mass regardless of where they come from).

The discretized mass fluxes are

$$F_{i;n}^{+\leftarrow} = D\rho_{i+1;n} / \Delta x + f_{i;n}^{+\leftarrow}; \quad F_{i;n}^{+\rightarrow} = D\rho_{i;n} / \Delta x + f_{i;n}^{+\rightarrow}, \tag{7}$$

$$F_{i;n}^{-\leftarrow} = D\rho_{i;n} / \Delta x + f_{i;n}^{-\leftarrow}; \quad F_{i;n}^{-\rightarrow} = D\rho_{i-1;n} / \Delta x + f_{i;n}^{-\rightarrow}, \tag{8}$$

where D is the diffusion coefficient and where $F_{i;n}^{+\leftarrow} = F_{i+1;n}^{-\leftarrow}$ and $F_{i;n}^{+\rightarrow} = F_{i+1;n}^{-\rightarrow}$. The correlations of the noise terms in (7) and (8) are given by

$$\langle f_{i;n}^{+\leftarrow} f_{j;m}^{+\leftarrow} \rangle = \frac{A_{i+1;n} \delta_{i,j} \delta_{n,m}}{2\Delta x \Delta t}, \quad \langle f_{i;n}^{-\rightarrow} f_{j;m}^{-\rightarrow} \rangle = \frac{A_{i-1;n} \delta_{i,j} \delta_{n,m}}{2\Delta x \Delta t} \tag{9}$$

and

$$\langle f_{i;n}^{+\rightarrow} f_{j;m}^{+\rightarrow} \rangle = \langle f_{i;n}^{-\leftarrow} f_{j;m}^{-\leftarrow} \rangle = \frac{A_{i;n} \delta_{i,j} \delta_{n,m}}{2\Delta x \Delta t}. \tag{10}$$

Analogous expressions hold for $f_{i;n}^{+\leftarrow} = f_{i+1;n}^{-\leftarrow}$ and $f_{i;n}^{+\rightarrow} = f_{i+1;n}^{-\rightarrow}$, with all other combinations being zero (e.g., $\langle f_{i;n}^{+\rightarrow} f_{j;n}^{+\leftarrow} \rangle = 0$). Note that this construction agrees with our previous formulation since

$$\langle f_{i;n}^+ f_{j;m}^+ \rangle = \langle f_{i;n}^{+\rightarrow} f_{j;m}^{+\rightarrow} \rangle + \langle f_{i;n}^{+\leftarrow} f_{j;m}^{+\leftarrow} \rangle = \frac{(A_{i;n} + A_{i+1;n}) \delta_{i,j} \delta_{n,m}}{2\Delta x \Delta t} \tag{11}$$

and

$$\langle f_{i;n}^- f_{j;m}^- \rangle = \langle f_{i;n}^{-\rightarrow} f_{j;m}^{-\rightarrow} \rangle + \langle f_{i;n}^{-\leftarrow} f_{j;m}^{-\leftarrow} \rangle = \frac{(A_{i;n} + A_{i-1;n}) \delta_{i,j} \delta_{n,m}}{2\Delta x \Delta t}. \tag{12}$$

Matching the variance of density fluctuations at equilibrium fixes the amplitude to be $A_{i;n} = 2D\rho_{i;n}$.

Substituting these expressions into (5) yields

$$\frac{\rho_{i;n+1} - \rho_{i;n}}{\Delta t} = D \frac{\rho_{i+1;n} + \rho_{i-1;n} - 2\rho_{i;n}}{\Delta x^2} - \frac{(f_{i;n}^{+\rightarrow} - f_{i;n}^{+\leftarrow}) - (f_{i;n}^{-\rightarrow} - f_{i;n}^{-\leftarrow})}{\Delta x}. \tag{13}$$

Using $f_{i;n}^{+\leftarrow} = f_{i+1;n}^{-\leftarrow}$ and $f_{i;n}^{+\rightarrow} = f_{i+1;n}^{-\rightarrow}$, this may be written as

$$\frac{\rho_{i;n+1} - \rho_{i;n}}{\Delta t} = D \frac{\rho_{i+1;n} + \rho_{i-1;n} - 2\rho_{i;n}}{\Delta x^2} - \left(\frac{f_{i;n}^{-\leftarrow} - f_{i+1;n}^{-\leftarrow}}{\Delta x} - \frac{f_{i-1;n}^{-\rightarrow} - f_{i;n}^{-\rightarrow}}{\Delta x} \right). \tag{14}$$

The steady state density, $\bar{\rho}_i$, is obtain from

$$D \frac{\bar{\rho}_{i+1} + \bar{\rho}_{i-1} - 2\bar{\rho}_i}{\Delta x^2} = 0 \tag{15}$$

which implies that it is linear.

The momentum fluxes are closely related to the mass fluxes. Specifically

$$G_{i,n}^{+ \leftarrow} = v_{i+1;n} F_{i,n}^{+ \leftarrow}; \quad G_{i,n}^{+ \rightarrow} = v_{i;n} F_{i,n}^{+ \rightarrow}; \quad G_{i,n}^{- \leftarrow} = v_{i;n} F_{i,n}^{- \leftarrow}; \quad G_{i,n}^{- \rightarrow} = v_{i-1;n} F_{i,n}^{- \rightarrow}. \tag{16}$$

As with the formulation for the density, we may write (6) as

$$\frac{P_{i,n+1} - P_{i;n}}{\Delta t} = D \frac{\rho_{i+1;n} v_{i+1;n} + \rho_{i-1;n} v_{i-1;n} - 2\rho_{i;n} v_{i;n}}{\Delta x^2} - \frac{(v_{i;n} f_{i,n}^{+ \rightarrow} - v_{i+1;n} f_{i,n}^{+ \leftarrow}) - (v_{i-1;n} f_{i,n}^{- \rightarrow} - v_{i;n} f_{i,n}^{- \leftarrow})}{\Delta x} \tag{17}$$

or

$$\frac{P_{i,n+1} - P_{i;n}}{\Delta t} = D \frac{\rho_{i+1;n} v_{i+1;n} + \rho_{i-1;n} v_{i-1;n} - 2\rho_{i;n} v_{i;n}}{\Delta x^2} - \left(\frac{v_{i;n} f_{i,n}^{- \leftarrow} - v_{i+1;n} f_{i+1;n}^{- \leftarrow}}{\Delta x} - \frac{v_{i-1;n} f_{i-1;n}^{+ \rightarrow} - v_{i;n} f_{i,n}^{+ \rightarrow}}{\Delta x} \right). \tag{18}$$

Since $\bar{p}_i = \bar{\rho}_i \bar{v}_i$, the steady-state momentum is linear and $\bar{v}_i = \bar{p}_i / \bar{\rho}_i$ is linear if the density is constant.

These discrete equations take the following continuous form as $\Delta x, \Delta t \rightarrow 0$

$$\frac{\partial \rho}{\partial t} = D \frac{\partial^2 \rho}{\partial x^2} + \frac{\partial f^{- \leftarrow}}{\partial x} - \frac{\partial f^{+ \rightarrow}}{\partial x}, \quad \frac{\partial p}{\partial t} = D \frac{\partial^2 \rho v}{\partial x^2} + \frac{\partial v f^{- \leftarrow}}{\partial x} - \frac{\partial v f^{+ \rightarrow}}{\partial x}. \tag{19}$$

If we define $f = f^{+ \rightarrow} - f^{- \leftarrow}$ then

$$\frac{\partial \rho}{\partial t} = D \frac{\partial^2 \rho}{\partial x^2} - \frac{\partial f}{\partial x}, \quad \frac{\partial p}{\partial t} = D \frac{\partial^2 \rho v}{\partial x^2} - \frac{\partial v f}{\partial x}. \tag{20}$$

Using $p = \rho v$, we obtain the following equation for velocity:

$$\rho \frac{\partial v}{\partial t} = 2D \frac{\partial \rho}{\partial x} \frac{\partial v}{\partial x} + D \rho \frac{\partial^2 v}{\partial x^2} - \frac{\partial v f}{\partial x}. \tag{21}$$

Note that when $f \equiv 0$ and the density is constant, this equation reduces to

$$\frac{\partial v}{\partial t} = D \frac{\partial^2 v}{\partial x^2} \tag{22}$$

which gives the linear Navier–Stokes equation for shear flow.

Finally, we may use Eq. (14) to formulate the numerical scheme

$$\rho_{i,n+1} = \rho_{i;n} + \frac{D\Delta t}{\Delta x^2} (\rho_{i+1;n} + \rho_{i-1;n} - 2\rho_{i;n}) + \frac{\Delta t}{\Delta x} (f_{i+1;n}^{- \leftarrow} - f_{i;n}^{- \leftarrow} - f_{i;n}^{+ \rightarrow} + f_{i-1;n}^{+ \rightarrow}), \tag{23}$$

where the stochastic terms are evaluated numerically using

$$f_{i,n}^{- \leftarrow} = \sqrt{\frac{D\rho_{i;n}}{\Delta x \Delta t}} \mathfrak{R}_{i;n}, \quad f_{i,n}^{+ \rightarrow} = \sqrt{\frac{D\rho_{i;n}}{\Delta x \Delta t}} \mathfrak{R}'_{i;n}, \tag{24}$$

where $\mathfrak{R}_{i;n}$ and $\mathfrak{R}'_{i;n}$ are independent, Gaussian distributed, random variables with zero mean and unit variance. Similarly, for momentum

$$P_{i,n+1} = P_{i;n} + \frac{D\Delta t}{\Delta x^2} (\rho_{i+1;n} v_{i+1;n} + \rho_{i-1;n} v_{i-1;n} - 2\rho_{i;n} v_{i;n}) + \frac{\Delta t}{\Delta x} (v_{i+1;n} f_{i+1;n}^{- \leftarrow} - v_{i;n} f_{i,n}^{- \leftarrow} - v_{i;n} f_{i,n}^{+ \rightarrow} + v_{i-1;n} f_{i-1;n}^{+ \rightarrow}). \tag{25}$$

Note that this numerical scheme is a generalization of that presented in [19]. In the deterministic case ($f = 0$) the scheme is known as forward-time-centered-space (FTCS) and has a maximum stable time step of $\Delta t_{\max} = \Delta x^2 / 2D$ [29].

Finally, we note that for the purpose of implementing an Algorithm Refinement hybrid, as presented in Section 5, it is useful to formulate the numerical schemes above as

$$\rho_{i;n+1} = \rho_{i;n} - \frac{\Delta t}{\Delta x} \left[(F_{i;n}^{+\rightarrow} - F_{i;n}^{+\leftarrow}) - (F_{i;n}^{-\rightarrow} - F_{i;n}^{-\leftarrow}) \right], \tag{26}$$

$$p_{i;n+1} = p_{i;n} - \frac{\Delta t}{\Delta x} \left[(G_{i;n}^{+\rightarrow} - G_{i;n}^{+\leftarrow}) - (G_{i;n}^{-\rightarrow} - G_{i;n}^{-\leftarrow}) \right], \tag{27}$$

where the fluxes are given by Eqs. (7), (8), and (16).

4. Correlations of fluctuations

The discretized construction of the previous section may be used to obtain the equal-time correlations of fluctuations $\langle \delta\rho_i\delta\rho_j \rangle$, $\langle \delta\rho_i\delta v_j \rangle$, and $\langle \delta v_i\delta v_j \rangle$. First, consider the density correlation; taking Eq. (23), we may write an expression for the density fluctuation $\delta\rho_i = \rho_{i;n} - \bar{\rho}_i$ as

$$\delta\rho'_i = \delta\rho_i + \frac{D\Delta t}{\Delta x^2} (\delta\rho_{i+1} + \delta\rho_{i-1} - 2\delta\rho_i) + \frac{\Delta t}{\Delta x} (f_i^{+\leftarrow} - f_i^{+\rightarrow} - f_i^{-\leftarrow} + f_i^{-\rightarrow}), \tag{28}$$

where prime indicates the new value at $n + 1$. We square both sides and take an average to get

$$\langle \delta\rho'_i\delta\rho'_i \rangle = \langle \delta\rho_i\delta\rho_i \rangle + T_1^{\rho\rho} + T_2^{\rho\rho} + T_3^{\rho\rho}, \tag{29}$$

where $T_1^{\rho\rho}$, $T_2^{\rho\rho}$, and $T_3^{\rho\rho}$ are given by (45) in Appendix A.

Expression (29) may be used as the basis for a relaxation scheme [29] to evaluate $\langle \delta\rho_i\delta\rho_j \rangle$. In the limit $\Delta t \rightarrow 0$ the terms of $O(\mathcal{C}^2)$, where $\mathcal{C} = D\Delta t/\Delta x^2$, vanish and the correlation of the density fluctuations may be obtained by directly solving $T_1^{\rho\rho} + T_3^{\rho\rho} = 0$, or

$$\begin{aligned} & (\langle \delta\rho_i\delta\rho_{j+1} \rangle + \langle \delta\rho_i\delta\rho_{j-1} \rangle + \langle \delta\rho_{i+1}\delta\rho_j \rangle + \langle \delta\rho_{i-1}\delta\rho_j \rangle - 4\langle \delta\rho_i\delta\rho_j \rangle) \\ & + \frac{1}{\Delta x} ((\bar{\rho}_{i+1} + \bar{\rho}_{i-1} + 2\bar{\rho}_i)\delta_{i,j} - (\bar{\rho}_{i+1} + \bar{\rho}_i)\delta_{i+1,j} - (\bar{\rho}_{i-1} + \bar{\rho}_i)\delta_{i-1,j}) = 0 \end{aligned} \tag{30}$$

giving $\langle \delta\rho_i\delta\rho_j \rangle = \bar{\rho}_i\delta_{ij}/\Delta x$ as may be verified by direct substitution. For finite Δt , the result obtained from relaxation of the full expression is not much different (see Fig. 2).

Next we consider the density–velocity correlation. The starting point is to identify $\delta p_i = p_{i;n} - \bar{p}_i = \bar{\rho}_i\delta v_i + \bar{v}_i\delta\rho_i$ and write (25) as

$$\begin{aligned} \delta\rho'_j\bar{v}_j + \bar{\rho}_j\delta v'_j &= \delta\rho_j\bar{v}_j + \bar{\rho}_j\delta v_j + \frac{D\Delta t}{\Delta x^2} (\bar{v}_{j+1}\delta\rho_{j+1} + \bar{v}_{j-1}\delta\rho_{j-1} - 2\bar{v}_j\delta\rho_j) + \frac{D\Delta t}{\Delta x^2} (\bar{\rho}_{j+1}\delta v_{j+1} + \bar{\rho}_{j-1}\delta v_{j-1} - 2\bar{\rho}_j\delta v_j) \\ &+ \frac{\Delta t}{\Delta x} (\bar{v}_{j+1}f_j^{+\leftarrow} - \bar{v}_jf_j^{+\rightarrow} - \bar{v}_jf_j^{-\leftarrow} + \bar{v}_{j-1}f_j^{-\rightarrow}). \end{aligned} \tag{31}$$

Taking the product of the above expression with (28) and averaging gives

$$\bar{v}_j\langle \delta\rho'_i\delta\rho'_j \rangle + \bar{\rho}_j\langle \delta\rho'_i\delta v'_j \rangle = \bar{v}_j\langle \delta\rho_i\delta\rho_j \rangle + \bar{\rho}_j\langle \delta\rho_i\delta v_j \rangle + T_1^{\rho v} + T_2^{\rho v} + T_3^{\rho v} + T_4^{\rho v} + T_5^{\rho v} + T_6^{\rho v}, \tag{32}$$

where $T_l^{\rho v}$ ($l = 1, \dots, 6$) are given by (46) in Appendix A. Taking $\langle \delta\rho'_i\delta\rho'_j \rangle = \langle \delta\rho_i\delta\rho_j \rangle$ as given

$$\langle \delta\rho'_i\delta v'_j \rangle = \langle \delta\rho_i\delta v_j \rangle + \frac{1}{\bar{\rho}_j} (T_1^{\rho v} + T_2^{\rho v} + T_3^{\rho v} + T_4^{\rho v} + T_5^{\rho v} + T_6^{\rho v}) \tag{33}$$

which may be solved numerically by iterative relaxation to obtain $\langle \delta\rho_i\delta v_j \rangle$. In the limit $\Delta t \rightarrow 0$ the above simplifies to $T_1^{\rho v} + T_2^{\rho v} + T_3^{\rho v} + T_6^{\rho v} = 0$ which may be written as

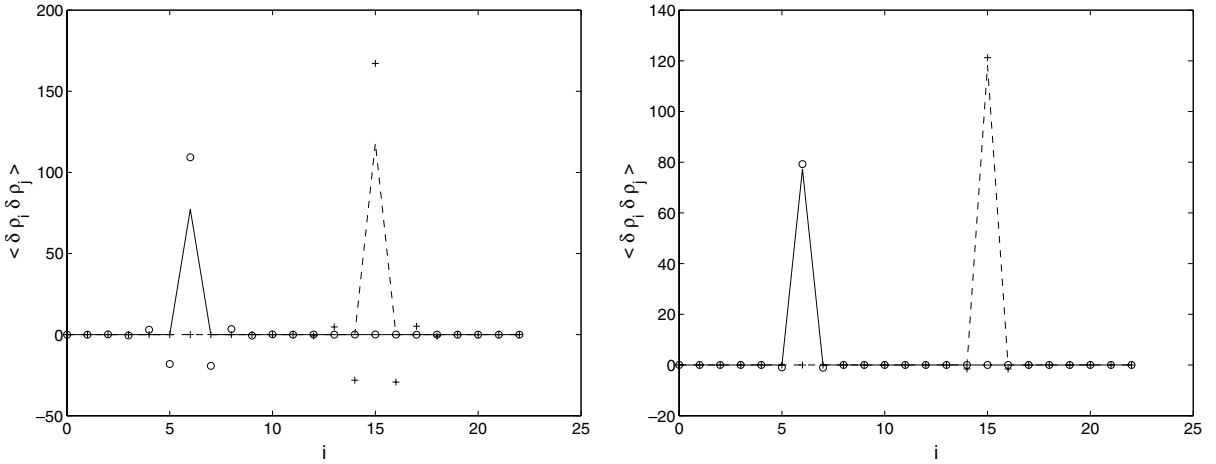


Fig. 2. Density correlation $\langle \rho_i \rho_j \rangle$ as function of i for $j = 6$ (circles) and $j = 15$ (crosses) as from (29) for a linear density gradient ($\rho_0 = 50, \rho_{M+1} = 150$). Left graph is $\Delta t = \Delta t_{\max}/2$; right is $\Delta t = \Delta t_{\max}/20$. In limit $\Delta t \rightarrow 0$ correlation $\langle \delta \rho_i \delta \rho_j \rangle = (\bar{\rho}_i / \Delta x) \delta_{ij}$ (solid and dashed lines). Parameters are: $D = 1, \Delta x = 1, M = 21, \Delta t_{\max} = \Delta x^2 / 2D$.

$$\begin{aligned} & \frac{\bar{\rho}_i \bar{v}_i}{\Delta x} (\delta_{i,j+1} + \delta_{i,j-1} - 2\delta_{i,j}) + (\bar{\rho}_{j+1} \langle \delta \rho_i \delta v_{j+1} \rangle + \bar{\rho}_{j-1} \langle \delta \rho_i \delta v_{j-1} \rangle - 2\bar{\rho}_j \langle \delta \rho_i \delta v_j \rangle) + \frac{\bar{v}_j \bar{\rho}_j}{\Delta x} (\delta_{i+1,j} + \delta_{i-1,j} - 2\delta_{i,j}) \\ & + \bar{\rho}_j (\langle \delta \rho_{i+1} \delta v_j \rangle + \langle \delta \rho_{i-1} \delta v_j \rangle - 2\langle \delta \rho_i \delta v_j \rangle) + \frac{1}{\Delta x} (\bar{v}_{j+1} \bar{\rho}_{i+1} \delta_{i,j} - \bar{v}_j \bar{\rho}_{i+1} \delta_{i+1,j} + \bar{v}_j \bar{\rho}_i \delta_{i,j} - \bar{v}_{j-1} \bar{\rho}_i \delta_{i+1,j} \\ & - \bar{v}_{j+1} \bar{\rho}_i \delta_{i-1,j} + \bar{v}_j \bar{\rho}_i \delta_{i,j} - \bar{v}_j \bar{\rho}_{i-1} \delta_{i-1,j} + \bar{v}_{j-1} \bar{\rho}_{i-1} \delta_{i,j}) = 0 \end{aligned} \tag{34}$$

which gives $\langle \delta \rho_i \delta v_j \rangle = 0$. For finite Δt there is a small, non-zero contribution which is associated with the truncation error of the numerical scheme. From Fig. 3, we see that this truncation error is $O(\Delta t)$.

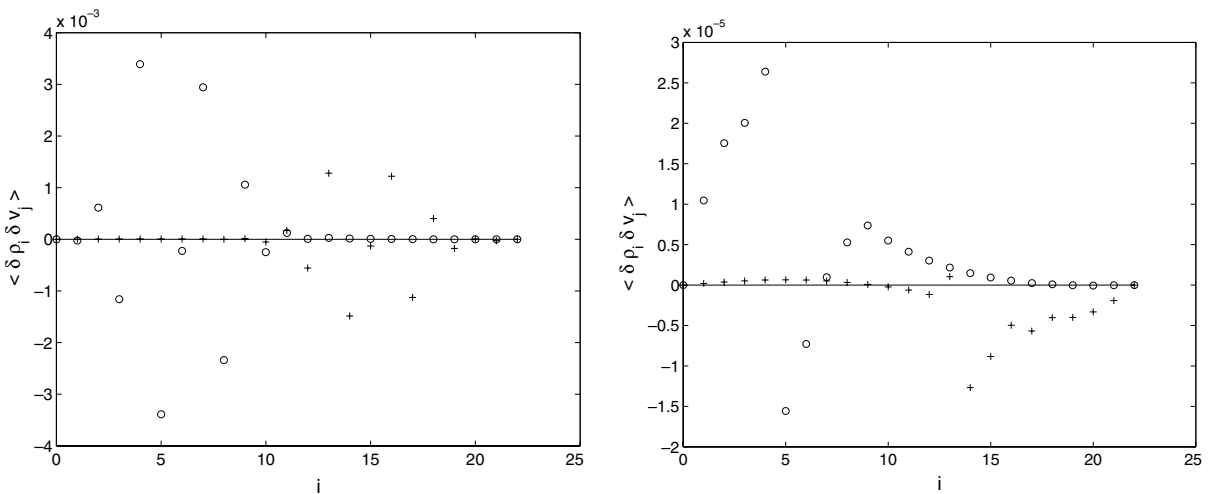


Fig. 3. Correlation $\langle \delta \rho_i \delta v_j \rangle$ for the boundary conditions $\rho_0 = 50, \rho_{M+1} = 150, v_0 = 0, v_{M+1} = 1$. Left graph is $\Delta t = \Delta t_{\max}/2$; right is $\Delta t = \Delta t_{\max}/20$. In limit $\Delta t \rightarrow 0$ correlation $\langle \delta \rho_i \delta v_j \rangle = 0$ (solid line). Parameters are as in Fig. 2.

Finally, let us evaluate the velocity–velocity correlation; the procedure is similar with the starting point of (31). The algebra is tedious but straight-forward. First, the left hand side is

$$\left\langle (\delta\rho'_i\bar{v}_i + \bar{\rho}_i\delta v'_i) (\delta\rho'_j\bar{v}_j + \bar{\rho}_j\delta v'_j) \right\rangle = \bar{v}_j\bar{v}_i\langle\delta\rho'_i\delta\rho'_j\rangle + \bar{\rho}_i\bar{\rho}_j\langle\delta v'_i\delta v'_j\rangle + \bar{v}_i\bar{\rho}_j\langle\delta\rho'_i\delta v'_j\rangle + \bar{\rho}_i\bar{v}_j\langle\delta v'_i\delta\rho'_j\rangle. \tag{35}$$

As before, we take $\langle\delta\rho'_i\delta\rho'_j\rangle = \langle\delta\rho_i\delta\rho_j\rangle$, cancelling this term on each side and similarly for the matching $\langle\delta\pi\rho\delta v\rangle$ terms that appear on both sides. The right hand side may be written as

$$\bar{v}_j\bar{v}_i\langle\delta\rho_i\delta\rho_j\rangle + \bar{\rho}_i\bar{\rho}_j\langle\delta v_i\delta v_j\rangle + \bar{v}_i\bar{\rho}_j\langle\delta\rho_i\delta v_j\rangle + \bar{\rho}_i\bar{v}_j\langle\delta v_i\delta\rho_j\rangle + \sum_{l=1}^8 T_l^{vv}, \tag{36}$$

where T_l^{vv} ($l = 1, \dots, 8$) are given by (47) in Appendix A. This gives us a relaxation expression

$$\langle\delta v'_i\delta v'_j\rangle = \langle\delta v_i\delta v_j\rangle + \frac{1}{\bar{\rho}_i\bar{\rho}_j} \sum_{l=1}^8 T_l^{vv}. \tag{37}$$

Results from relaxation are shown in Fig. 4. In the limit $\Delta t \rightarrow 0$, we may drop the terms T_3^{vv} , T_4^{vv} , T_6^{vv} , T_7^{vv} , and T_8^{vv} and write the remaining terms as

$$\begin{aligned} \langle\delta v'_i\delta v'_j\rangle = & \langle\delta v_i\delta v_j\rangle + \frac{\mathcal{C}}{\bar{\rho}_i\bar{\rho}_j} \left[\frac{1}{\Delta x} \bar{\rho}_i\bar{v}_i^2 (\delta_{i,j+1} + \delta_{i,j-1} - 2\delta_{i,j}) + \frac{1}{\Delta x} \bar{\rho}_j\bar{v}_j^2 (\delta_{i+1,j} + \delta_{i-1,j} - 2\delta_{i,j}) \right. \\ & + \bar{\rho}_i(\bar{\rho}_{j+1}\langle\delta v_i\delta v_{j+1}\rangle + \bar{\rho}_{j-1}\langle\delta v_i\delta v_{j-1}\rangle - 2\bar{\rho}_j\langle\delta v_i\delta v_j\rangle) + \bar{\rho}_j(\bar{\rho}_{i+1}\langle\delta v_{i+1}\delta v_j\rangle + \bar{\rho}_{i-1}\langle\delta v_{i-1}\delta v_j\rangle \\ & - 2\bar{\rho}_i\langle\delta v_i\delta v_j\rangle) + \frac{1}{\Delta x} (\bar{v}_{i+1}\bar{v}_{j+1}\bar{\rho}_{i+1}\delta_{i,j} - \bar{v}_{i+1}\bar{v}_j\bar{\rho}_{i+1}\delta_{i+1,j} + \bar{v}_i\bar{v}_j\bar{\rho}_i\delta_{i,j} - \bar{v}_i\bar{v}_{j-1}\bar{\rho}_i\delta_{i+1,j} - \bar{v}_i\bar{v}_{j+1}\bar{\rho}_i\delta_{i-1,j} \\ & \left. + \bar{v}_j\bar{v}_j\bar{\rho}_i\delta_{i,j} - \bar{v}_{i-1}\bar{v}_j\bar{\rho}_{i-1}\delta_{i-1,j} + \bar{v}_{i-1}\bar{v}_{j-1}\bar{\rho}_{i-1}\delta_{i,j}) \right]. \tag{38} \end{aligned}$$

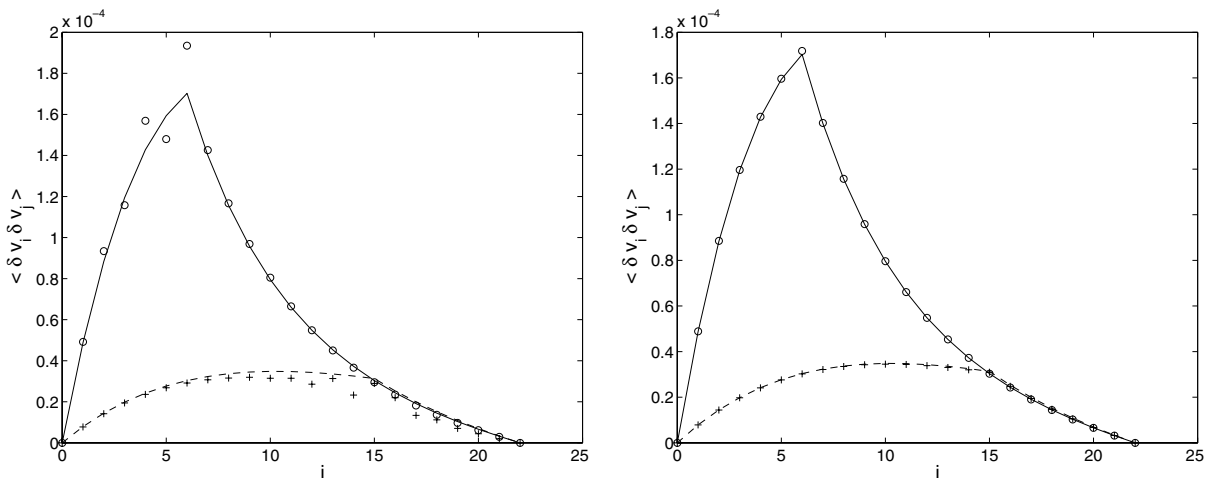


Fig. 4. Correlation $\langle\delta v_i\delta v_j\rangle$ obtained by relaxation; parameters are as in Fig. 3. Left graph is $\Delta t = \Delta t_{\max}/2$; right is $\Delta t = \Delta t_{\max}/20$. Result for limit $\Delta t \rightarrow 0$ are solid and dashed lines.

The expressions are still complicated but easily solved by relaxation yielding the results shown in Fig. 4 for the case of both density and velocity gradients. The case of only a velocity gradient the results are in perfect agreement with (3).

5. Algorithm refinement hybrid

The train model is most easily understood as a random walk model, which is how it is simulated as a particle system (see Section 2). As described in Section 3, the train model may also be simulated as a continuum system whose stochastic PDE is integrated in time by generating the deterministic and white-noise fluxes. We now consider how the two formulations may be coupled as a particle/continuum hybrid. As mentioned in the introduction, this type of hybrid computation that combines two distinctly different algorithmic approaches that model the same physical process is commonly known as AR. The present AR hybrid for the train model is validated by comparing with conventional particle and continuum simulations as well as with the predicted correlations obtained in the previous section.

Fig. 5 illustrates the geometry used in our AR hybrid with a particle simulation on the left side and a continuum computation on the right. For simplicity we take the continuum grid spacing, Δx , equal to the particle grid spacing (width of a train).

At the beginning of a time step, the particle region is extended by one grid point into the continuum region. This added “handshaking” region is filled with particles according to the density of the underlying grid point such that $\langle N_{I,n} \rangle = \rho_{I,n} \Delta x / m$. In addition, each particle is given the same velocity of the train, namely, v_I . All particles, in the handshaking region and elsewhere, are then evolved for a time Δt using the random walk dynamics outlined in Section 2. The total number and total momentum for particles jumping left and right across the interface are recorded and used in the continuum portion of the computation (see below). Any particles that move outside the particle region are removed from the simulation.

Once the particle update is complete, (7), (8), (16), and (24) are used to compute the density and momentum fluxes for each continuum grid point *except* for the grid point adjacent to the particle region. For that point, the fluxes recorded during the particles’ motion are used instead of

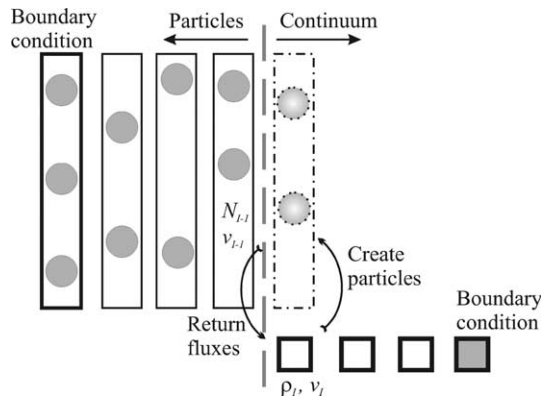


Fig. 5. Algorithm Refinement hybrid for the train model. The particle simulation is performed in the region on the left (from 0 to $I - 1$) and a PDE solver is used on the right (I to M); the methods are coupled at the interface. For the particle algorithm, new particles (open circles) are generated in the “handshaking” region (cell k) and at the Dirichlet boundary (left platform). For the continuum algorithm the fluxes $F_{I,n}^-$, $F_{I,n}^+$, $G_{I,n}^-$, and $G_{I,n}^+$ (i.e., between cells $I - 1$ and k) are obtained from the particle computation.

$F_{I,n}^{\leftarrow\leftarrow}$, $F_{I,n}^{\leftarrow}G_{I,n}^{\leftarrow\leftarrow}$, and $G_{I,n}^{\leftarrow\leftarrow}$. Given the fluxes, each continuum grid point is updated using (26) and (27), which completes one time step for the hybrid. Note that the coupling exactly conserves mass and momentum as the fluxes of these quantities across the interface are synchronized to be the same for the two algorithms.

The boundary conditions fix the density and velocity of the first and last grid point (i.e., a “platform”). When this grid point is simulated with particles, then it is a reservoir with particles immediately replenished (or removed) as they leave (or enter). We consider two cases: (1) a velocity gradient only and (2) both density and velocity gradients. The case of a density gradient only is equivalent to our earlier study [19] of simple diffusion. In both of the present cases there are long range correlations of the velocity fluctuations $\langle\delta v_i\delta v_j\rangle$, as shown in Section 4.

A variety of simulations were run to illustrate the performance of the AR hybrid. In all cases the simulations were executed 10^8 steps using a time step of $\Delta t = \Delta t_{\max}/20 = 0.025$. Both stochastic and non-stochastic (i.e., deterministic) PDE solvers were tested. In the former, the noise amplitude is computed using (24); in the latter, $f_{i,n}^{\pm\leftarrow} = 0$. The deterministic method is similar to that used earlier in particle/continuum hybrids for fluid mechanics (e.g., the DSMC/Euler hybrid in [3]).

First we consider the AR hybrid using a stochastic PDE solver. Fig. 6 shows that for the mean values of the density and velocity the simulations using a pure particle, a pure continuum, and the AR hybrid are all in excellent agreement with the expected results of a linear density profile and a velocity profile given by Eq. (2).

The correlation of velocity fluctuations is also in good agreement for all three numerical approaches; see Fig. 7 for the case of only a velocity gradient and Fig. 8 for the case of both a velocity and density gradient. These results indicate that the AR hybrid correctly captures the long-ranged nature of these non-equilibrium fluctuations. This is a significant result since these long-range correlations are generic to hydrodynamic systems out of global equilibrium [23].

We now consider the AR hybrid using a deterministic PDE solver. Again the mean values of the density and velocity for this hybrid are in perfect agreement with the theory (see Fig. 9). What is most interesting are the results for the correlation of velocity fluctuations shown in Fig. 10 for the case of

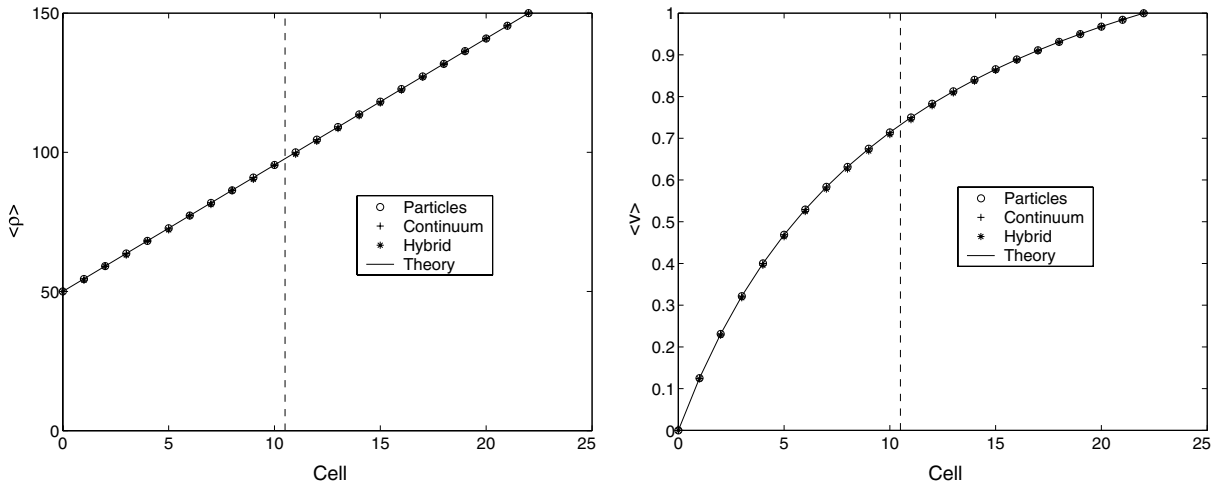


Fig. 6. Mean density (left) and velocity (right) as functions of position for a system of $M = 21$ trains with boundary conditions $\rho_0 = 50$, $\rho_{M+1} = 150$, $v_0 = 0$, and $v_{22} = 1$. Simulations are pure particle (circle), pure stochastic PDE (cross), and hybrid of particles/stochastic PDE (asterisk); theory (solid line) is linear density and Eq. (2). Dashed line indicates the interface location for the hybrid simulation.

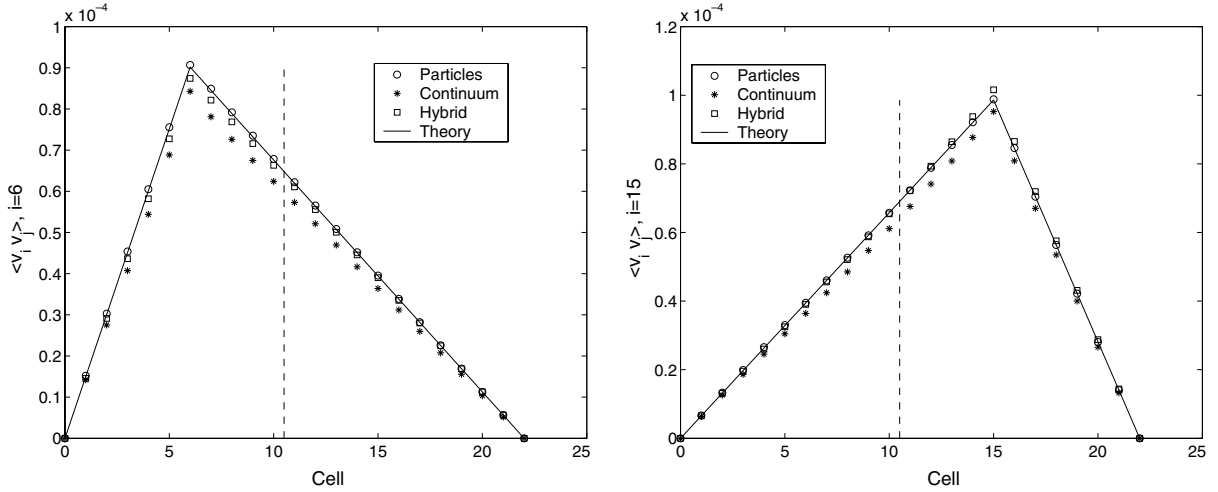


Fig. 7. Velocity–velocity correlation $\langle \delta v_i \delta v_j \rangle$ as functions of position i for $j = 6$ (left) and $j = 15$ (right). Parameters and symbols are as in Fig. 6 except that $\rho_0 = \rho_{M+1} = 100$ (i.e., velocity gradient only). Solid line is theoretical result given by (3).

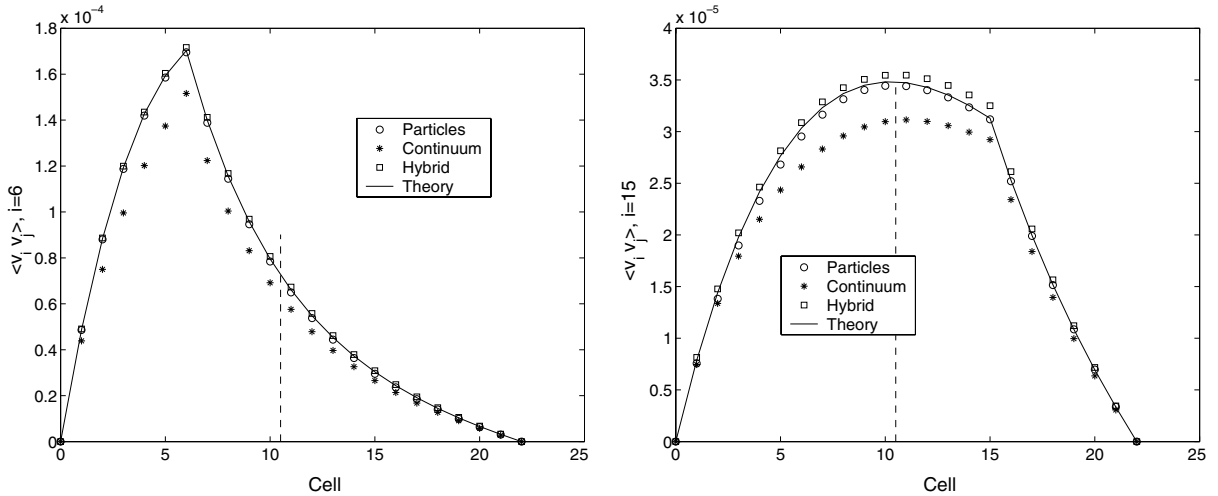


Fig. 8. Velocity–velocity correlation $\langle \delta \rho_i \delta \rho_j \rangle$ as functions of position i for $j = 6$ (left) and $j = 15$ (right). Parameters and symbols are as in Fig. 6. Solid line is theoretical result given by (38) solved by relaxation.

only a velocity gradient and Fig. 11 for the case of both a velocity and density gradient. The amplitude of the $\langle \delta v_i \delta v_j \rangle$ correlations is roughly reduced by half due to the absence of noise in half the system (i.e., the deterministic PDE side) yet the correlations are still long-ranged, spanning the length of the system.

This result is in contrast with the findings in our previous study [19] of linear diffusion in which we showed that the variance of density fluctuations, $\langle (\delta \rho_i)^2 \rangle$, went quickly to zero in the deterministic region of the simulation. However, there is no contradiction since the long-range nature of hydrodynamic correlations is not due to the presence of noise throughout the system. Rather, it is the hydrodynamic transport that propagates the correlation and this transport is correctly computed by the hybrid, as demonstrated by

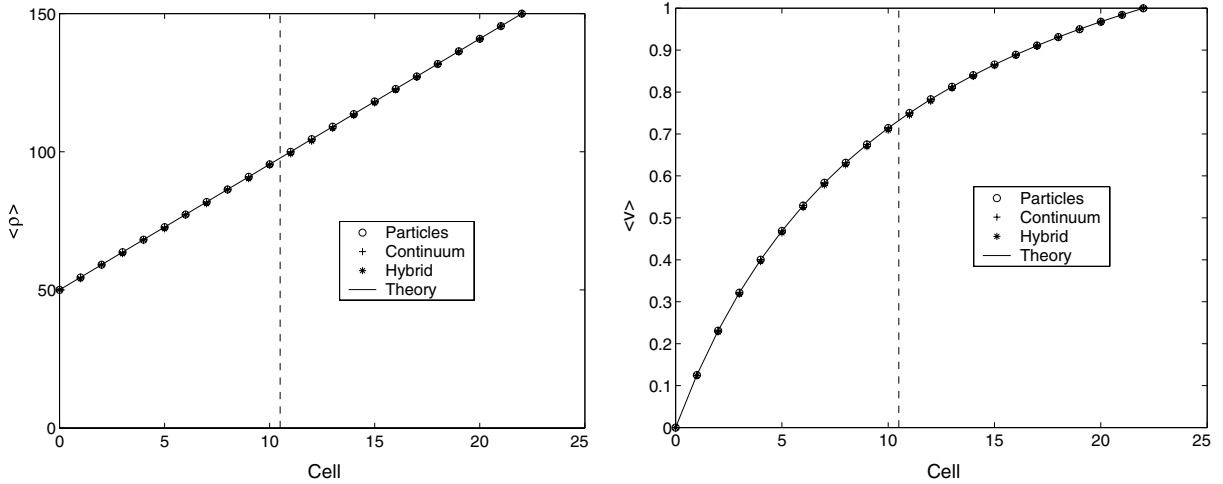


Fig. 9. Mean density (left) and velocity (right) as functions of position; same as Fig. 6 except hybrid uses a deterministic PDE solver for the right-hand side of the system.

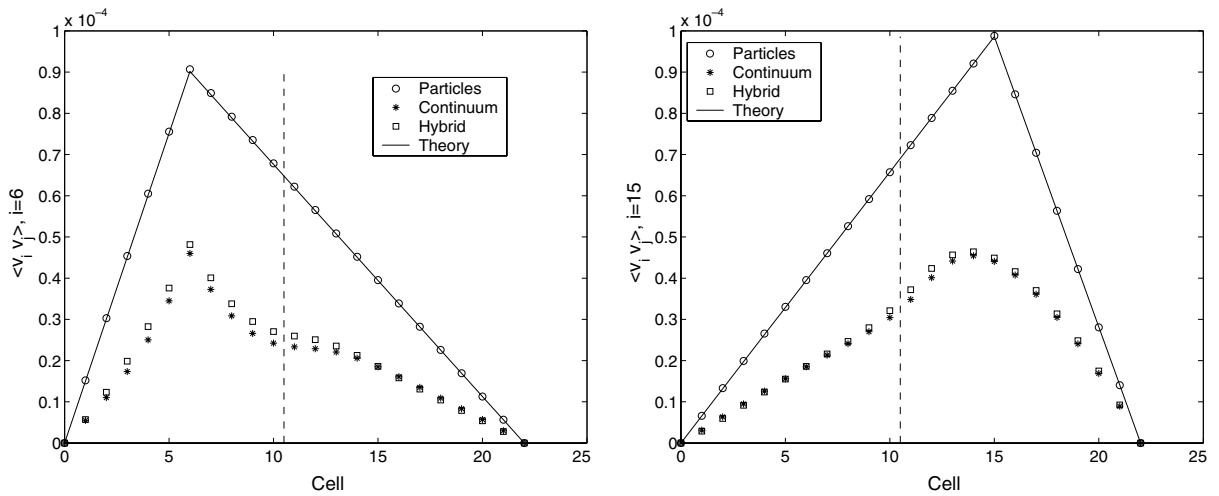


Fig. 10. Velocity–velocity correlation $\langle \delta v_i \delta v_j \rangle$ as functions of position i for $j=6$ (left) and $j=15$ (right). Hybrid uses a deterministic PDE solver for the right-hand side of the system; all else is as in Fig. 7.

the correct profiles of mean density and velocity shown in Fig. 9. In other words, local fluctuations are produced in the particle region and propagated by the hydrodynamic transport, which in the train model is purely viscous, to produce the correlations.

In brief, the effect of long-ranged correlations is still present, albeit at a reduced amplitude, even if only one part of the hybrid is stochastic. On one hand, this result is good news since it means that even when using a deterministic PDE solver, which is far more commonly the case for AR hybrids, some of the qualitative features of long-ranged correlations are preserved. On the other hand, a reduction (or for that matter, an enhancement) of the fluctuations by a factor of two can lead to a greatly altered time-dependent behavior. This is a serious concern for modelling noise-driven phenomena where fluctuations and their

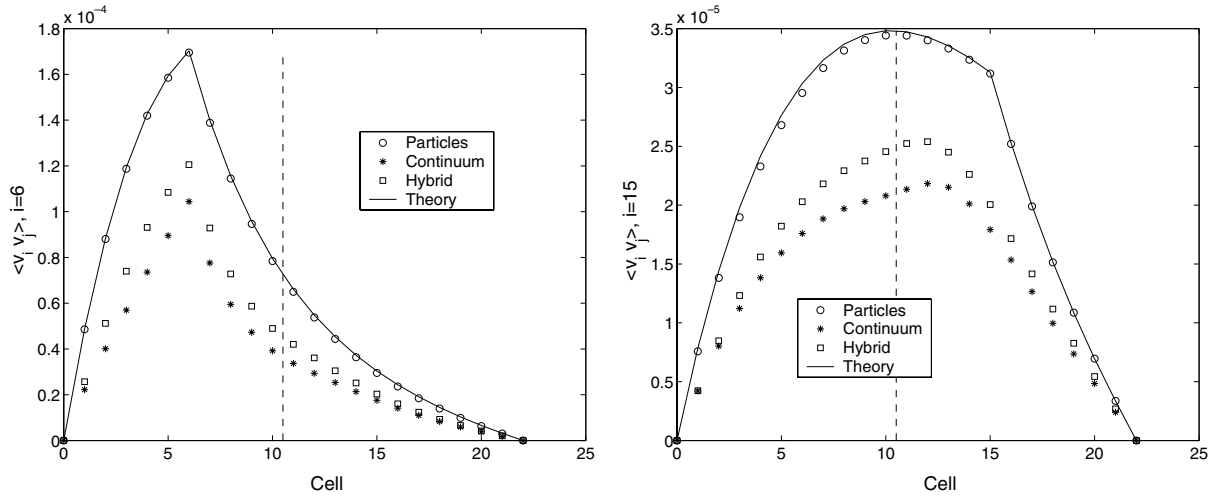


Fig. 11. Velocity–velocity correlation $\langle \delta v_i \delta v_j \rangle$ as functions of position i for $j=6$ (left) and $j=15$ (right). Hybrid uses a deterministic PDE solver for the right-hand side of the system; all else is as in Fig. 8.

correlations are often exponentially amplified (first-passage time problems, spontaneous transitions at unstable points, explosive ignition, etc.). Clearly, the nature of the physical process and the relative importance of fluctuations to the correct modelling of that process govern the construction of stochastic and deterministic Algorithm Refinement hybrids.

6. Concluding remarks

In this paper we investigate an Algorithm Refinement hybrid of a simple hydrodynamic model. Our study focused on static (i.e., equal-time) correlations of velocity fluctuations since they are long-ranged when the system is out of equilibrium, a generic feature of fluctuating hydrodynamics [23]. Hybrids that capture static correlations correctly are expected to do well in reproducing dynamic correlations since the latter are given by the former plus hydrodynamic transport. That said, it would still be interesting to confirm this expectation by measuring time dependent correlations in AR hybrids and comparing the results with pure particle systems. For some physical problems generating time dependent fluctuations and correlations correctly will be crucial for accuracy.

Our future work will focus on strongly non-linear systems. We are currently investigating an AR hybrid that combines the fluctuating Navier–Stokes equations with direct simulation Monte Carlo (DSMC). Besides the long-range correlations of the form considered in the present work, there are hydrodynamic correlations *perpendicular* to imposed gradients [25] that can be measured to verify the accuracy of the scheme. Another way to test the accuracy of this hybrid would be to measure the statistical properties of hydrodynamic instabilities (e.g., onset time for Rayleigh–Benard convection) and validate the results by comparison with a pure DSMC simulation. Parallel to this work we are investigating AR hybrids for the time-dependent Ginzburg–Landau equation (and variants). As the physical problems, mathematical models, and numerical schemes become increasingly more complex and non-linear, it becomes increasingly evident how important it is to establish a foundation based on simple systems such as the random walk.

Acknowledgments

The authors thank G.L. Eyink and M. Malek-Mansour for helpful discussions. This work was performed at Los Alamos National Laboratory under the auspices of the National Nuclear Security Agency of US Department of Energy (LA-UR-04-3794) under Grant KC-07-01-01.

Appendix A. Details of correlation calculation

To evaluate the expressions for the correlations one makes use of the relations

$$\langle \delta\rho_i f_j^{\pm\leftrightarrow} \rangle = \langle \delta v_i f_j^{\pm\leftrightarrow} \rangle = \langle f_i^{\pm\leftarrow} f_j^{\pm\rightarrow} \rangle = \langle f_i^{\pm\leftarrow} f_j^{\mp\rightarrow} \rangle = 0. \tag{39}$$

The variances of the stochastic fluxes out of i are

$$\langle f_i^{+\rightarrow} f_j^{+\rightarrow} \rangle = \langle f_i^{-\leftarrow} f_j^{-\leftarrow} \rangle = \frac{D\bar{\rho}_i \delta_{i,j}}{\Delta x \Delta t}. \tag{40}$$

The other variances are found using the relations

$$f_{i-1}^{+\rightarrow} = f_i^{-\leftarrow}; \quad f_i^{+\rightarrow} = f_{i+1}^{-\leftarrow}; \quad f_{i-1}^{+\leftarrow} = f_i^{-\rightarrow}; \quad f_i^{+\leftarrow} = f_{i+1}^{-\rightarrow}, \tag{41}$$

so

$$\langle f_i^{+\leftarrow} f_j^{+\leftarrow} \rangle = \frac{D\bar{\rho}_{i+1} \delta_{i,j}}{\Delta x \Delta t}; \quad \langle f_i^{-\rightarrow} f_j^{-\rightarrow} \rangle = \frac{D\bar{\rho}_{i-1} \delta_{i,j}}{\Delta x \Delta t}, \tag{42}$$

$$\langle f_i^{+\leftarrow} f_j^{-\leftarrow} \rangle = \frac{D\bar{\rho}_{i+1} \delta_{i+1,j}}{\Delta x \Delta t}; \quad \langle f_i^{-\rightarrow} f_j^{+\leftarrow} \rangle = \frac{D\bar{\rho}_i \delta_{i-1,j}}{\Delta x \Delta t}, \tag{43}$$

$$\langle f_i^{+\rightarrow} f_j^{-\rightarrow} \rangle = \frac{D\bar{\rho}_i \delta_{i+1,j}}{\Delta x \Delta t}; \quad \langle f_i^{-\leftarrow} f_j^{+\rightarrow} \rangle = \frac{D\bar{\rho}_{i-1} \delta_{i-1,j}}{\Delta x \Delta t}. \tag{44}$$

Finally, the boundary conditions are $\langle \delta\rho_0 \delta\rho_j \rangle = \langle \delta\rho_{M+1} \delta\rho_j \rangle = 0$ since the platforms are at fixed mean density with equal-time fluctuations that are independent of the fluctuations in the rest of the system.

The terms $T_1^{\rho\rho}$, $T_2^{\rho\rho}$, and $T_3^{\rho\rho}$ in (29) are given by

$$\begin{aligned} T_1^{\rho\rho} &= \left\langle \delta\rho_i \left(\frac{D\Delta t}{\Delta x^2} (\delta\rho_{j+1} + \delta\rho_{j-1} - 2\delta\rho_j) \right) \right\rangle + \left\langle \delta\rho_j \left(\frac{D\Delta t}{\Delta x^2} (\delta\rho_{i+1} + \delta\rho_{i-1} - 2\delta\rho_i) \right) \right\rangle \\ &= \mathcal{C} (\langle \delta\rho_i \delta\rho_{j+1} \rangle + \langle \delta\rho_i \delta\rho_{j-1} \rangle + \langle \delta\rho_{i+1} \delta\rho_j \rangle + \langle \delta\rho_{i-1} \delta\rho_j \rangle - 4\langle \delta\rho_i \delta\rho_j \rangle), \end{aligned} \tag{45a}$$

$$\begin{aligned} T_2^{\rho\rho} &= \left\langle \left(\frac{D\Delta t}{\Delta x^2} (\delta\rho_{i+1} + \delta\rho_{i-1} - 2\delta\rho_i) \right) \left(\frac{D\Delta t}{\Delta x^2} (\delta\rho_{j+1} + \delta\rho_{j-1} - 2\delta\rho_j) \right) \right\rangle \\ &= \mathcal{C}^2 (\langle \delta\rho_{i+1} \delta\rho_{j+1} \rangle + \langle \delta\rho_{i-1} \delta\rho_{j+1} \rangle - 2\langle \delta\rho_i \delta\rho_{j+1} \rangle + \langle \delta\rho_{i+1} \delta\rho_{j-1} \rangle + \langle \delta\rho_{i-1} \delta\rho_{j-1} \rangle \\ &\quad - 2\langle \delta\rho_i \delta\rho_{j-1} \rangle - 2\langle \delta\rho_{i+1} \delta\rho_j \rangle - 2\langle \delta\rho_{i-1} \delta\rho_j \rangle + 4\langle \delta\rho_i \delta\rho_j \rangle), \end{aligned} \tag{45b}$$

and

$$\begin{aligned} T_3^{\rho\rho} &= \left\langle \left(-\frac{\Delta t}{\Delta x} (f_i^{+\leftarrow} - f_i^{+\rightarrow} - f_i^{-\leftarrow} + f_i^{-\rightarrow}) \right) \left(-\frac{\Delta t}{\Delta x} (f_j^{+\leftarrow} - f_j^{+\rightarrow} - f_j^{-\leftarrow} + f_j^{-\rightarrow}) \right) \right\rangle \\ &= \frac{\mathcal{C}}{\Delta x} ((\bar{\rho}_{i+1} + \bar{\rho}_{i-1} + 2\bar{\rho}_i) \delta_{i,j} - (\bar{\rho}_{i+1} + \bar{\rho}_i) \delta_{i+1,j} - (\bar{\rho}_{i-1} + \bar{\rho}_i) \delta_{i-1,j}), \end{aligned} \tag{45c}$$

where $\mathcal{C} = D\Delta t / \Delta x^2$.

The terms $T_l^{\rho v}$ ($l = 1, \dots, 6$) in (33) are given by

$$\begin{aligned} T_1^{\rho v} &= \frac{D\Delta t}{\Delta x^2} \langle \delta\rho_i (\bar{v}_{j+1} \delta\rho_{j+1} + \bar{v}_{j-1} \delta\rho_{j-1} - 2\bar{v}_j \delta\rho_j) \rangle \\ &= \mathcal{C} (\bar{v}_{j+1} \langle \delta\rho_i \delta\rho_{j+1} \rangle + \bar{v}_{j-1} \langle \delta\rho_i \delta\rho_{j-1} \rangle - 2\bar{v}_j \langle \delta\rho_i \delta\rho_j \rangle), \end{aligned} \quad (46a)$$

$$\begin{aligned} T_2^{\rho v} &= \frac{D\Delta t}{\Delta x^2} \langle \delta\rho_i (\bar{\rho}_{j+1} \delta v_{j+1} + \bar{\rho}_{j-1} \delta v_{j-1} - 2\bar{\rho}_j \delta v_j) \rangle \\ &= \mathcal{C} (\bar{\rho}_{j+1} \langle \delta\rho_i \delta v_{j+1} \rangle + \bar{\rho}_{j-1} \langle \delta\rho_i \delta v_{j-1} \rangle - 2\bar{\rho}_j \langle \delta\rho_i \delta v_j \rangle), \end{aligned} \quad (46b)$$

$$\begin{aligned} T_3^{\rho v} &= \frac{D\Delta t}{\Delta x^2} \langle (\delta\rho_{i+1} + \delta\rho_{i-1} - 2\delta\rho_i) (\delta\rho_j \bar{v}_j + \bar{\rho}_j \delta v_j) \rangle \\ &= \mathcal{C} \bar{v}_j (\langle \delta\rho_{i+1} \delta\rho_j \rangle + \langle \delta\rho_{i-1} \delta\rho_j \rangle - 2\langle \delta\rho_i \delta\rho_j \rangle) + \mathcal{C} \bar{\rho}_j (\langle \delta\rho_{i+1} \delta v_j \rangle + \langle \delta\rho_{i-1} \delta v_j \rangle - 2\langle \delta\rho_i \delta v_j \rangle), \end{aligned} \quad (46c)$$

$$\begin{aligned} T_4^{\rho v} &= \left(\frac{D\Delta t}{\Delta x^2} \right)^2 \langle (\delta\rho_{i+1} + \delta\rho_{i-1} - 2\delta\rho_i) (\bar{v}_{j+1} \delta\rho_{j+1} + \bar{v}_{j-1} \delta\rho_{j-1} - 2\bar{v}_j \delta\rho_j) \rangle \\ &= \mathcal{C}^2 \{ \bar{v}_{j+1} (\langle \delta\rho_{i+1} \delta\rho_{j+1} \rangle + \langle \delta\rho_{i-1} \delta\rho_{j+1} \rangle - 2\langle \delta\rho_i \delta\rho_{j+1} \rangle) + \bar{v}_{j-1} (\langle \delta\rho_{i+1} \delta\rho_{j-1} \rangle \\ &\quad + \langle \delta\rho_{i-1} \delta\rho_{j-1} \rangle - 2\langle \delta\rho_i \delta\rho_{j-1} \rangle) - 2\bar{v}_j (\langle \delta\rho_{i+1} \delta\rho_j \rangle + \langle \delta\rho_{i-1} \delta\rho_j \rangle - 2\langle \delta\rho_i \delta\rho_j \rangle) \}, \end{aligned} \quad (46d)$$

$$\begin{aligned} T_5^{\rho v} &= \left(\frac{D\Delta t}{\Delta x^2} \right)^2 \langle (\delta\rho_{i+1} + \delta\rho_{i-1} - 2\delta\rho_i) (\bar{\rho}_{j+1} \delta v_{j+1} + \bar{\rho}_{j-1} \delta v_{j-1} - 2\bar{\rho}_j \delta v_j) \rangle \\ &= \mathcal{C}^2 \{ \bar{\rho}_{j+1} (\langle \delta\rho_{i+1} \delta v_{j+1} \rangle + \langle \delta\rho_{i-1} \delta v_{j+1} \rangle - 2\langle \delta\rho_i \delta v_{j+1} \rangle) + \bar{\rho}_{j-1} (\langle \delta\rho_{i+1} \delta v_{j-1} \rangle \\ &\quad + \langle \delta\rho_{i-1} \delta v_{j-1} \rangle - 2\langle \delta\rho_i \delta v_{j-1} \rangle) - 2\bar{\rho}_j (\langle \delta\rho_{i+1} \delta v_j \rangle + \langle \delta\rho_{i-1} \delta v_j \rangle - 2\langle \delta\rho_i \delta v_j \rangle), \end{aligned} \quad (46e)$$

and

$$\begin{aligned} T_6^{\rho v} &= \left(\frac{\Delta t}{\Delta x} \right)^2 \langle (f_i^{+\leftarrow} - f_i^{+\rightarrow} - f_i^{-\leftarrow} + f_i^{-\rightarrow}) (\bar{v}_{j+1} f_j^{+\leftarrow} - \bar{v}_j f_j^{+\rightarrow} - \bar{v}_j f_j^{-\leftarrow} + \bar{v}_{j-1} f_j^{-\rightarrow}) \rangle \\ &= \frac{\mathcal{C}}{\Delta x} (\bar{v}_{j+1} \bar{\rho}_{i+1} \delta_{i,j} - \bar{v}_j \bar{\rho}_{i+1} \delta_{i+1,j} + \bar{v}_j \bar{\rho}_i \delta_{i,j} - \bar{v}_{j-1} \bar{\rho}_i \delta_{i+1,j} - \bar{v}_{j+1} \bar{\rho}_i \delta_{i-1,j} \\ &\quad + \bar{v}_j \bar{\rho}_i \delta_{i,j} - \bar{v}_j \bar{\rho}_{i-1} \delta_{i-1,j} + \bar{v}_{j-1} \bar{\rho}_{i-1} \delta_{i,j}). \end{aligned} \quad (46f)$$

Finally, the terms in (36) are given by

$$\begin{aligned} T_1^{vv} &= \left\langle (\delta\rho_i \bar{v}_i) \left(\frac{D\Delta t}{\Delta x^2} (\bar{v}_{j+1} \delta\rho_{j+1} + \bar{v}_{j-1} \delta\rho_{j-1} - 2\bar{v}_j \delta\rho_j) \right) \right\rangle \\ &\quad + \left\langle (\delta\rho_j \bar{v}_j) \left(\frac{D\Delta t}{\Delta x^2} (\bar{v}_{i+1} \delta\rho_{i+1} + \bar{v}_{i-1} \delta\rho_{i-1} - 2\bar{v}_i \delta\rho_i) \right) \right\rangle \\ &= \mathcal{C} \bar{v}_i (\langle \bar{v}_{j+1} \delta\rho_i \delta\rho_{j+1} \rangle + \langle \bar{v}_{j-1} \delta\rho_i \delta\rho_{j-1} \rangle - 2\bar{v}_j \langle \delta\rho_i \delta\rho_j \rangle) \\ &\quad + \mathcal{C} \bar{v}_j (\langle \bar{v}_{i+1} \delta\rho_i \delta\rho_j \rangle + \langle \bar{v}_{i-1} \delta\rho_i \delta\rho_j \rangle - 2\bar{v}_i \langle \delta\rho_i \delta\rho_j \rangle), \end{aligned} \quad (47a)$$

$$\begin{aligned}
 T_2^{vv} &= \left\langle (\bar{\rho}_i \delta v_i) \left(\frac{D\Delta t}{\Delta x^2} (\bar{\rho}_{j+1} \delta v_{j+1} + \bar{\rho}_{j-1} \delta v_{j-1} - 2\bar{\rho}_j \delta v_j) \right) \right\rangle \\
 &\quad + \left\langle (\bar{\rho}_j \delta v_j) \left(\frac{D\Delta t}{\Delta x^2} (\bar{\rho}_{i+1} \delta v_{i+1} + \bar{\rho}_{i-1} \delta v_{i-1} - 2\bar{\rho}_i \delta v_i) \right) \right\rangle \\
 &= \mathcal{C} \bar{\rho}_i (\bar{\rho}_{j+1} \langle \delta v_i \delta v_{j+1} \rangle + \bar{\rho}_{j-1} \langle \delta v_i \delta v_{j-1} \rangle - 2\bar{\rho}_j \langle \delta v_i \delta v_j \rangle) + \mathcal{C} \bar{\rho}_j (\bar{\rho}_{i+1} \langle \delta v_{i+1} \delta v_j \rangle + \bar{\rho}_{i-1} \langle \delta v_{i-1} \delta v_j \rangle \\
 &\quad - 2\bar{\rho}_i \langle \delta v_i \delta v_j \rangle), \tag{47b}
 \end{aligned}$$

$$\begin{aligned}
 T_3^{vv} &= \left\langle \left(\frac{D\Delta t}{\Delta x^2} (\bar{v}_{i+1} \delta \rho_{i+1} + \bar{v}_{i-1} \delta \rho_{i-1} - 2\bar{v}_i \delta \rho_i) \right) \left(\frac{D\Delta t}{\Delta x^2} (\bar{v}_{j+1} \delta \rho_{j+1} + \bar{v}_{j-1} \delta \rho_{j-1} - 2\bar{v}_j \delta \rho_j) \right) \right\rangle \\
 &= \mathcal{C}^2 \bar{v}_{i+1} (\bar{v}_{j+1} \langle \delta \rho_{i+1} \delta \rho_{j+1} \rangle + \bar{v}_{j-1} \langle \delta \rho_{i+1} \delta \rho_{j-1} \rangle - 2\bar{v}_j \langle \delta \rho_{i+1} \delta \rho_j \rangle) + \mathcal{C}^2 \bar{v}_{i-1} (\bar{v}_{j+1} \langle \delta \rho_{i-1} \delta \rho_{j+1} \rangle \\
 &\quad + \bar{v}_{j-1} \langle \delta \rho_{i-1} \delta \rho_{j-1} \rangle - 2\bar{v}_j \langle \delta \rho_{i-1} \delta \rho_j \rangle) - 2\mathcal{C}^2 \bar{v}_i (\bar{v}_{j+1} \langle \delta \rho_i \delta \rho_{j+1} \rangle + \bar{v}_{j-1} \langle \delta \rho_i \delta \rho_{j-1} \rangle - 2\bar{v}_j \langle \delta \rho_i \delta \rho_j \rangle), \tag{47c}
 \end{aligned}$$

$$\begin{aligned}
 T_4^{vv} &= \left\langle \left(\frac{D\Delta t}{\Delta x^2} (\bar{\rho}_{i+1} \delta v_{i+1} + \bar{\rho}_{i-1} \delta v_{i-1} - 2\bar{\rho}_i \delta v_i) \right) \left(\frac{D\Delta t}{\Delta x^2} (\bar{\rho}_{j+1} \delta v_{j+1} + \bar{\rho}_{j-1} \delta v_{j-1} - 2\bar{\rho}_j \delta v_j) \right) \right\rangle \\
 &= \mathcal{C}^2 \bar{\rho}_{i+1} (\bar{\rho}_{j+1} \langle \delta v_{i+1} \delta v_{j+1} \rangle + \bar{\rho}_{j-1} \langle \delta v_{i+1} \delta v_{j-1} \rangle - 2\bar{\rho}_j \langle \delta v_{i+1} \delta v_j \rangle) + \mathcal{C}^2 \bar{\rho}_{i-1} (\bar{\rho}_{j+1} \langle \delta v_{i-1} \delta v_{j+1} \rangle \\
 &\quad + \bar{\rho}_{j-1} \langle \delta v_{i-1} \delta v_{j-1} \rangle - 2\bar{\rho}_j \langle \delta v_{i-1} \delta v_j \rangle) - 2\mathcal{C}^2 \bar{\rho}_i (\bar{\rho}_{j+1} \langle \delta v_i \delta v_{j+1} \rangle + \bar{\rho}_{j-1} \langle \delta v_i \delta v_{j-1} \rangle - 2\bar{\rho}_j \langle \delta v_i \delta v_j \rangle), \tag{47d}
 \end{aligned}$$

$$\begin{aligned}
 T_5^{vv} &= \left\langle \left(\frac{\Delta t}{\Delta x} (\bar{v}_{i+1} f_i^{+\leftarrow} - \bar{v}_i f_i^{+\rightarrow} - \bar{v}_i f_i^{-\leftarrow} + \bar{v}_{i-1} f_i^{-\rightarrow}) \right) \left(\frac{\Delta t}{\Delta x} (\bar{v}_{j+1} f_j^{+\leftarrow} - \bar{v}_j f_j^{+\rightarrow} - \bar{v}_j f_j^{-\leftarrow} + \bar{v}_{j-1} f_j^{-\rightarrow}) \right) \right\rangle \\
 &= \frac{\mathcal{C}}{\Delta x} (\bar{v}_{i+1} \bar{v}_{j+1} \bar{\rho}_{i+1} \delta_{i,j} - \bar{v}_{i+1} \bar{v}_j \bar{\rho}_{i+1} \delta_{i+1,j} + \bar{v}_i \bar{v}_j \bar{\rho}_i \delta_{i,j} - \bar{v}_i \bar{v}_{j-1} \bar{\rho}_i \delta_{i+1,j} - \bar{v}_i \bar{v}_{j+1} \bar{\rho}_i \delta_{i-1,j} + \bar{v}_i \bar{v}_j \bar{\rho}_i \delta_{i,j} \\
 &\quad - \bar{v}_{i-1} \bar{v}_j \bar{\rho}_{i-1} \delta_{i-1,j} + \bar{v}_{i-1} \bar{v}_{j-1} \bar{\rho}_{i-1} \delta_{i,j}), \tag{47e}
 \end{aligned}$$

$$\begin{aligned}
 T_6^{vv} &= \left\langle (\bar{\rho}_i \delta v_i) \left(\frac{D\Delta t}{\Delta x^2} (\bar{v}_{j+1} \delta \rho_{j+1} + \bar{v}_{j-1} \delta \rho_{j-1} - 2\bar{v}_j \delta \rho_j) \right) \right\rangle \\
 &\quad + \left\langle (\bar{\rho}_j \delta v_j) \left(\frac{D\Delta t}{\Delta x^2} (\bar{v}_{i+1} \delta \rho_{i+1} + \bar{v}_{i-1} \delta \rho_{i-1} - 2\bar{v}_i \delta \rho_i) \right) \right\rangle \\
 &= \mathcal{C} \bar{\rho}_i ((\bar{v}_{j+1} \langle \delta \rho_{j+1} \delta v_i \rangle + \bar{v}_{j-1} \langle \delta \rho_{j-1} \delta v_i \rangle - 2\bar{v}_j \langle \delta \rho_j \delta v_i \rangle)) \\
 &\quad + \mathcal{C} \bar{\rho}_j ((\bar{v}_{i+1} \langle \delta \rho_{i+1} \delta v_j \rangle + \bar{v}_{i-1} \langle \delta \rho_{i-1} \delta v_j \rangle - 2\bar{v}_i \langle \delta \rho_i \delta v_j \rangle)), \tag{47f}
 \end{aligned}$$

$$\begin{aligned}
 T_7^{vv} &= \left\langle (\bar{v}_i \delta \rho_i) \left(\frac{D\Delta t}{\Delta x^2} (\bar{\rho}_{j+1} \delta v_{j+1} + \bar{\rho}_{j-1} \delta v_{j-1} - 2\bar{\rho}_j \delta v_j) \right) \right\rangle \\
 &\quad + \left\langle (\bar{v}_j \delta \rho_j) \left(\frac{D\Delta t}{\Delta x^2} (\bar{\rho}_{i+1} \delta v_{i+1} + \bar{\rho}_{i-1} \delta v_{i-1} - 2\bar{\rho}_i \delta v_i) \right) \right\rangle \\
 &= \mathcal{C} \bar{v}_i (\bar{\rho}_{j+1} \langle \delta \rho_i \delta v_{j+1} \rangle + \bar{\rho}_{j-1} \langle \delta \rho_i \delta v_{j-1} \rangle - 2\bar{\rho}_j \langle \delta \rho_i \delta v_j \rangle) + \mathcal{C} \bar{v}_j (\bar{\rho}_{i+1} \langle \delta \rho_j \delta v_{i+1} \rangle + \bar{\rho}_{i-1} \langle \delta \rho_j \delta v_{i-1} \rangle \\
 &\quad - 2\bar{\rho}_i \langle \delta \rho_j \delta v_i \rangle), \tag{47g}
 \end{aligned}$$

$$\begin{aligned}
T_8^{vv} &= \left\langle \left(\frac{D\Delta t}{\Delta x^2} (\bar{v}_{i+1} \delta \rho_{i+1} + \bar{v}_{i-1} \delta \rho_{i-1} - 2\bar{v}_i \delta \rho_i) \right) \left(\frac{D\Delta t}{\Delta x^2} (\bar{\rho}_{j+1} \delta v_{j+1} + \bar{\rho}_{j-1} \delta v_{j-1} - 2\bar{\rho}_j \delta v_j) \right) \right\rangle \\
&\quad + (\text{same with } i \leftrightarrow j) \\
&= \mathcal{C}^2 \bar{v}_{i+1} (\bar{\rho}_{j+1} \langle \delta \rho_{i+1} \delta v_{j+1} \rangle + \bar{\rho}_{j-1} \langle \delta \rho_{i+1} \delta v_{j-1} \rangle - 2\bar{\rho}_j \langle \delta \rho_{i+1} \delta v_j \rangle) + \mathcal{C}^2 \bar{v}_{i-1} (\bar{\rho}_{j+1} \langle \delta \rho_{i-1} \delta v_{j+1} \rangle \\
&\quad + \bar{\rho}_{j-1} \langle \delta \rho_{i-1} \delta v_{j-1} \rangle - 2\bar{\rho}_j \langle \delta \rho_{i-1} \delta v_j \rangle) - 2\mathcal{C}^2 \bar{v}_i (\bar{\rho}_{j+1} \langle \delta \rho_i \delta v_{j+1} \rangle + \bar{\rho}_{j-1} \langle \delta \rho_i \delta v_{j-1} \rangle - 2\bar{\rho}_j \langle \delta \rho_i \delta v_j \rangle) \\
&\quad + (\text{same with } i \leftrightarrow j). \tag{47h}
\end{aligned}$$

Appendix B. Errata for Part I

In [19], Eq. (13) should read

$$f_{i;n}^+ = f_{i+1;n}^- = \sqrt{\frac{A_{i;n} + A_{i+1;n}}{2\Delta x \Delta t}} \mathfrak{R}_{i;n}.$$

References

- [1] D.C. Wadsworth, D.A. Erwin, One-dimensional hybrid continuum/particle simulation approach for rarefied hypersonic flows, AIAA Paper (1990) 90-1690.
- [2] P. Le Tallec, F. Mallinger, Coupling Boltzmann and Navier–Stokes equations by half fluxes, J. Comput. Phys. 136 (1997) 51.
- [3] A.L. Garcia, J.B. Bell, Wm.Y. Crutchfield, B.J. Alder, Adaptive mesh and algorithm refinement using direct simulation Monte Carlo, J. Comput. Phys. 154 (1999) 134.
- [4] O. Aktas, N.R. Aluru, A combined continuum/DSMC technique for multiscale analysis of microfluidic filters, J. Comput. Phys. 178 (2002) 342.
- [5] Q.H. Sun, I.D. Boyd, G.V. Candler, A hybrid continuum/particle approach for modeling subsonic, rarefied gas flows, J. Comput. Phys. 194 (2004) 256.
- [6] S.T. O’Connell, P.A. Thompson, Molecular dynamics–continuum hybrid computations: a tool for studying complex fluid flows, Phys. Rev. E 52 (1995) R5792.
- [7] N. Hadjiconstantinou, A. Patera, Heterogeneous atomistic–continuum representations for dense fluid systems, Int. J. Mod. Phys. C 8 (1997) 967.
- [8] E.G. Flekkoy, G. Wagner, J. Feder, Hybrid model for combined particle and continuum dynamics, Europhys. Lett. 52 (2000) 271.
- [9] R. Delgado-Buscalioni, P.V. Coveney, Continuum-particle hybrid coupling for mass, momentum, and energy transfers in unsteady fluid flow, Phys. Rev. E 67 (2003) 046704.
- [10] X. Nie, S. Chen, W. E, M. Robbins, A continuum and molecular dynamics hybrid method for micro- and nano-fluid flow, J. Fluid Mech. 500 (2004) 55.
- [11] F.F. Abraham, J.Q. Broughton, N. Bernstein, E. Kaxiras, Spanning the length scales in dynamic simulation, Comput. Phys. 12 (1998) 538.
- [12] V.B. Shenoy, R. Miller, E.B. Tadmor, D. Rodney, R. Phillips, M. Ortiz, An adaptive finite element approach to atomic-scale mechanics – the quasicontinuum method, J. Mech. Phys. Solids 47 (1999) 611.
- [13] R.E. Rudd, J.Q. Broughton, Concurrent coupling of length scales in solid state systems, Phys. Status Solidi B 217 (2000) 251.
- [14] G.J. Wagner, W.K. Liu, Coupling of atomistic and continuum simulations using a bridging scale decomposition, J. Comput. Phys. 190 (2003) 249.
- [15] T.P. Schulze, P. Smereka, W. E, Coupling kinetic Monte-Carlo and continuum models with application to epitaxial growth, J. Comput. Phys. 189 (2003) 197.
- [16] E. Moro, Hybrid method for simulating front propagation in reaction-diffusion systems, Phys. Rev. E 69 (2004) 060101.
- [17] C.W. Gardiner, Handbook of Stochastic Methods, second ed., Springer, Berlin, 1985.
- [18] A.L. Garcia, M. Malek Mansour, G. Lie, E. Clementi, Numerical integration of the fluctuating hydrodynamic equations, J. Stat. Phys. 47 (1987) 209.
- [19] F. Alexander, A. Garcia, D. Tartakovsky, Algorithm refinement for stochastic partial differential equations: I. linear diffusion, J. Comput. Phys. 182 (2002) 47–66.

- [20] J.M. Haile, *Molecular Dynamics Simulation*, Wiley, New York, 1992.
- [21] H. Spohn, Long range correlations for stochastic lattice gases in a nonequilibrium steady state, *J. Phys. A* 16 (1983) 4275.
- [22] A. Garcia, Long range thermal correlations in a knudsen flow system, *Phys. Lett.* 119 (1987) 379.
- [23] R. Schmitz, Fluctuations in nonequilibrium fluids, *Phys. Rep.* 171 (1988) 1.
- [24] A. Garcia, M. Malek Mansour, G. Lie, E. Clementi, Hydrodynamic fluctuations in a fluid under constant shear, *Phys. Rev. A* 36 (1987) 4348.
- [25] J.M. Ortiz de Zarate, J.V. Sengers, On the physical origin of long-ranged fluctuations in fluids in thermal nonequilibrium states, *J. Stat. Phys.* 115 (2004) 1341.
- [26] P. Ehrenfest, T. Ehrenfest, *The Conceptual Foundations of the Statistical Approach in Mechanics*, Cornell University Press, Ithaca, NY, 1959.
- [27] H.S. Robertson, *Statistical Thermophysics*, Prentice-Hall, Englewood Cliffs, NJ, 1993.
- [28] F. Baras, M. Malek Mansour, A. Garcia, A simple model for nonequilibrium fluctuations in a fluid, *Am. J. Phys.* 64 (1996) 1488.
- [29] A.L. Garcia, *Numerical Methods for Physics*, Prentice-Hall, Upper Saddle River, NJ, 2000.